A Multi-Resolution Dynamic Model for Face Aging Simulation

Jinli Suo
GUCAS
jlsuo.lhi@gmail.com

Feng Min Songchun Zhu
Lotus Hill Institute
fmin.lhi,sczhu.lhi@gmail.com

Shiguang Shan Xilin Chen
GUCAS
sgshan,xlchen@jdl.ac.cn

Abstract

In this paper we present a dynamic model for simulating face aging process. We adopt a high resolution grammatical face model[1] and augment it with age and hair features. This model represents all face images by a multi-layer And-Or graph and integrates three most prominent aspects related to aging changes: global appearance changes in hair style and shape, deformations and aging effects of facial components, and wrinkles appearance at various facial zones. Then face aging is modeled as a dynamic Markov process on this graph representation which is learned from a large dataset. Given an input image, we firstly compute the graph representation, and then sample the graph structures over various age groups according to the learned dynamic model. Finally we generate new face images with the sampled graphs. Our approach has three novel aspects: (1) the aging model is learned from a dataset of 50,000 adult faces at different ages; (2) we explicitly model the uncertainty in face aging and can sample multiple plausible aged faces for an input image; and (3) we conduct a simple human experiment to validate the simulated aging process.

1. Introduction

Face aging is an interesting and challenging problem in computer vision. Aging can cause significant alterations in face appearance, and deteriorate the performance of face recognition systems. Modeling face aging can help build more robust face recognition systems in a variety of real world applications, such as person identification based on old ID photos, recognition of fugitives, looking for missing children, and entertainment. Compared with other face modeling tasks, modeling face aging has some unique challenges. (i) There are large shape and texture variations over long term period, say 20-50 years. (ii) The perceived face age often depends on global non-facial factors, such as hair color and style, the degree of boldness of the forehead, and cultural and ethnic groups. (iii) It is very difficult to have face images of the same person over a long time period.

Human face aging has attracted research in computer vi-

sion, psychology, and computer graphics. Previous work on face aging can be divided into two categories: child growth and adult aging.

For **child growth**, shape change of face profile is the most prominent factor. Most researchers adopted coordinate transformation on a set of landmark points[3, 6] or a parametric approach[2, 13] to simulate age related shape changes. For example, Ramanathan and Challeppa[4] use parameters from anthropometric studies[22, 23] to define the deformation of facial landmarks in child growth. They also studied face verification problem across age progression[5]. For **adult aging**, both texture and shape change. In computer vision, most aging approaches are based on image examples, rather than physics. Burt[8, 9] studied two factors affecting age perception of adult faces – shape and color. From the average face image at different ages they extract average aging patterns and propose an aging approach. Several other approaches performed texture transferring from senior faces to young faces[10, 11, 12]. Some vision approaches have also been proposed for the age estimation[15, 16, 20, 21]. Some recent work adopted PCA approach to build a statistical model for the aging simulation, which includes[7, 26, 27]. In computer graphics, people mostly used physical model to simulate the changes in face aging. For example, Wu [16, 17] used a skin model to simulate the wrinkles on face as age increases. Berg [19] simulated the aging process of orbicularies muscles. Other similar work include [14] and [18]. The biggest disadvantage of these physical models is their complexity, which makes it difficult to generate photo-realistic aging effects.

In summary, the example based models are often limited by the small dataset, and the physical models are usually too complex to render realistic aged faces. Therefore, it is necessary to have a more sophisticated model to account for all factors involved in face aging, as well as a quantitative study on the intrinsic variabilities in face aging.

Motivated by these problems, we make the following contributions in this paper.

(1) We adopt a high resolution grammatical face model[1] to account for the large variations of the facial structures (different types of eyes, noses, mouths etc.), and
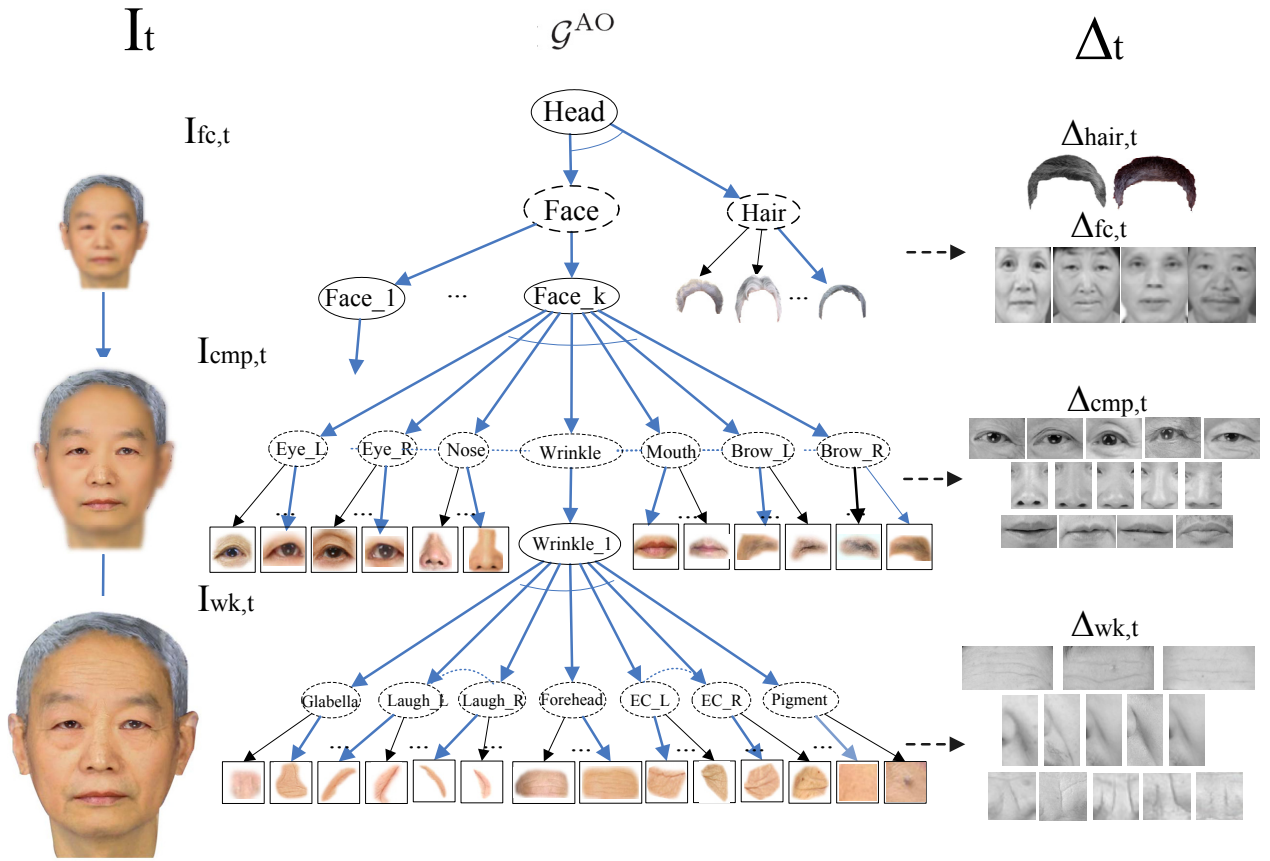
Figure 1. A high resolution face image I_t at age group t is represented in three resolutions – $I_{fc,t}$, $I_{cmp,t}$ and $I_{wk,t}$ (left) All face images at an age group are represented collectively a hierarchic And-Or graph $\mathcal{G}_t^{AO}$ (middle). The And nodes (in solid ellipses) in the graph $\mathcal{G}_t^{AO}$ represent coarse-to-fine decomposition of a face image into its parts and components. The Or-nodes (in dashed ellipses) represent alternative configurations. By choosing the Or-nodes, we obtain an And-graph G_t for a specific face instance. On the right side are their corresponding dictionaries $\Delta_{rc,t}$, $\Delta_{cmp,t}$ and $\Delta_{wk,t}$.

augment it with age and hair features. This generative model represents all face images by a multi-layer And-Or graph and integrates three most prominent aspects related to aging changes: global appearance changes in hair style and shape, deformations and aging effects of facial components, and wrinkle appearance in various facial zones.

(2) We adopt a dynamic Markov (motion) process on this graph representation for face aging. Given an input image, we first infer the graph representation, and then sample the graph structures over various age groups following the learned dynamic model. The sampled graphs then generate new images as plausible aged faces. We generate more sample faces for longer period to account for the uncertainty.

(3) We train the generative model and the dynamics based on a large dataset of 50,000 face images which are manually divided into different age groups and annotated into hairs and facial components. Thus the model is learned across many individuals over ages, because it is hard to get photos of the same person over long period.

(4) We conduct a simple human experiment to validate the simulated aging process.

The paper is organized in the following way. In Section 2 we formulate the layered face model and the dynamic models. Section 3 discusses the algorithms. Section 4 presents the experiments and some quantitative study. We conclude the paper discussion in Section 5.

2. Representation and formulation

In this section, we formulate the multi-resolution face representation and the dynamic model.

2.1. Multiscale graph for face modeling

We extend a multi-resolution grammatical model for face representation[1]. As Fig.1 illustrates, a face image I_t at age group t is represented in three resolutions, from coarse-to-fine,

$$I_t = (I_{fc,t}, I_{cmp,t}, I_{wk,t}).$$

$I_{fc,t}$ is the whole face image for general shape, hair style, skin color etc. $I_{cmp,t}$ refines the facial components (eyes, eyebrows, nose, mouth etc.). $I_{wk,t}$ further refines the wrinkles, skin marks, and pigments in different zones of the face.

All faces in age group t are collectively represented by an And-Or graph $\mathcal{G}_t^{\mathrm{AO}}$ (see the middle column of Fig.1) where an And-node (in solid ellipse) represents the decomposition and an Or-node (in dashed ellipse) represents the alternatives, for example, different eye shapes.

A dictionary Δ_t for each age group t is shown on the right side for various components over the three scales.

$$\Delta_t = \{\{\Delta_{hair,t}, \Delta_{fc,t}\}, \Delta_{cmp,t}, \Delta_{wk,t}\} \qquad (1)$$

where both $\Delta_{hair,t}$ and $\Delta_{fc,t}$ belong to the first resolution. This dictionary is learned from a large dataset for each individual age group separately. In latter sections, we use i as the index for the three resolutions.

After choosing the alternatives at the Or-nodes, the And-Or graph $\mathcal{G}_t^{\mathrm{AO}}$ becomes an And-graph G_t as a specific face instance. G_t in turn generates image I_t.

$$G_t \overset{\Delta_t}{\Longrightarrow} I_t \qquad (2)$$

We denote the set of faces produced by $\mathcal{G}_t^{\mathrm{AO}}$ as

$$\Sigma_t = \{G_t : G_t \subset \mathcal{G}^{\mathrm{AO}}\} \qquad (3)$$

Σ_t is a very large set of face images at age group t to account for the variabilities and composition. It is much larger than the training set.

The And-Or graph is a generative model that accounts for a large variety of faces.

In summary, the face representation is

$$G_t = (w_{1,t}, w_{2,t}, w_{3,t}). \qquad (4)$$

where $w_{i,t}$ are the hidden variables controlling the generation of I_t at different resolution layers. It can be further decomposed as

$$w_{i,t} = \{l_{i,t}, T_{i,t}^{geo}, T_{i,t}^{pht}\} \qquad (5)$$

where $l_{i,t}$ is a switch variable for the alternatives in the Or-nodes. $T_{i,k}^{geo}$ and $T_{i,k}^{pht}$ are the variables accounting for the photometric and geometric attributes of the components in the synthesized images.

We briefly present the image generation model in Eq.(6) for all the 3 scales according to the work in [1].

$$I_{i,t} = J_{i,t}^{rec}(w_{i,t}; \Delta_{i,t}) + I_{i,t}^{res}, i = 1, 2, 3. \qquad (6)$$

where $I_{i,t}^{res}$ is a residual image at time t with resolution i, which follows a Gaussian distribution.

The probabilistic model of the whole face can be written as

$$p(I_t | G_t; \Theta_{img,t}) = \prod_{i=1}^{3} p(I_{i,t} | w_{i,t}; \Delta_{i,t}) \qquad (7)$$
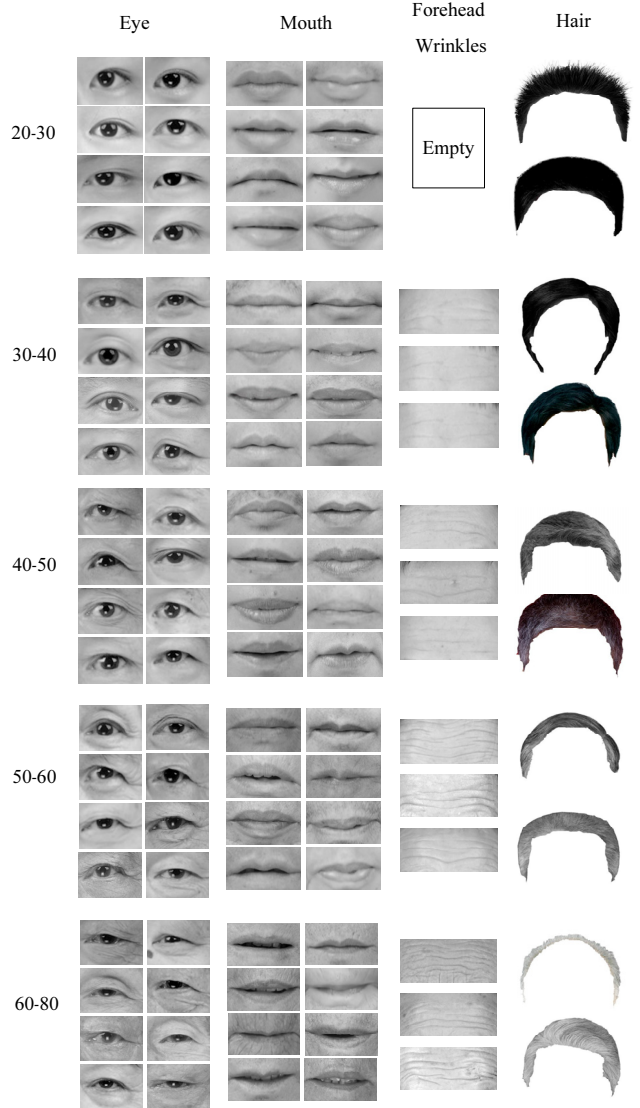

Figure 2. Examples of the facial components and hairs from the dictionaries of different age groups.

2.2. Modeling aging procedure as a Markov Chain

Markov Chain on graphs. As is known the future appearance of a subject depends only on the current appearance, therefore, face aging procedure can be modeled as a Markov Chain on Graph.

Fig.3 is an illustration of our dynamic model for graph motion[25]. I_1 is an input young face image and G_1 is its graph representation. I_2 to I_5 are four synthesized aged images in four consecutive age groups generated by G_2 to G_5. $\{G_1, G_2, ..., G_5\}$ is a graph chain describing face aging procedure.

There are two types of variations in the motion of Markov chain:

1) Continuous Variation. Some variations in the graph motion will only change the attributes(skin color, hair color,
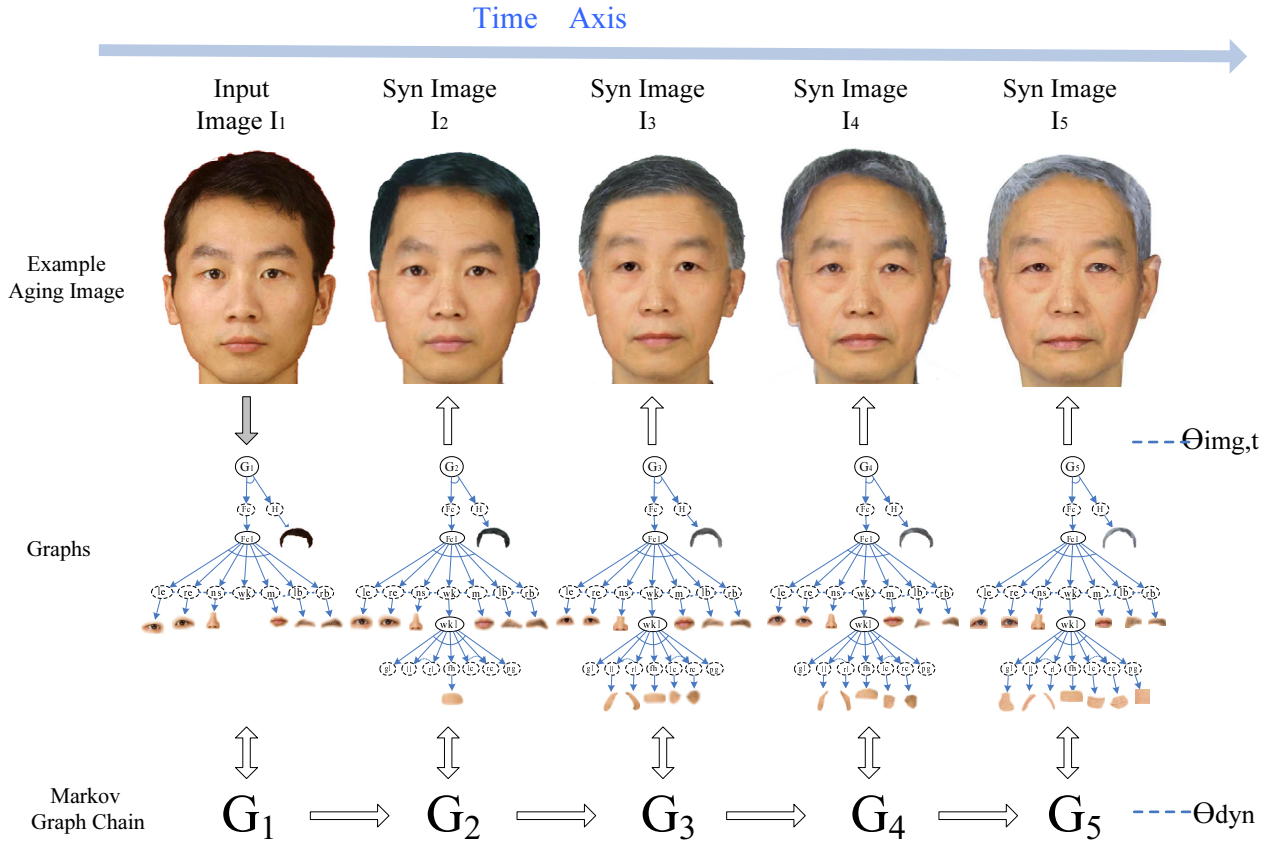
Figure 3. An aging process can be modeled by a Markov Chain on the And graphs G_t. The first row is a sequence of face images at different ages, the leftmost one is the input image, and the other four are synthesized aged images. The second row is the graph representations of the image sequence. Third row is the corresponding And-graphs G_t, which form a Markov Chain. $\Theta_{img,t}$ is the parameters for generating the images from G_t and Θ_{dyn} the parameters for aging progression.

wrinkle length etc.) of some Leaf-nodes. We represent them with the transition probability of $T_{i,t}^{geo}$ and $T_{i,t}^{pht}$.

2) Abrupt Variation. Some variations in the graph motion will change the topology of the graph. For example, new node inserted(wrinkles appear etc.) or the change of the alternatives in the Or-node(hair style changes etc.). We use the transition probabilities of $l_{i,t}$ to represent this variation.

For simplicity we assume that l, $T_{i,t}^{geo}$ and $T_{i,t}^{pht}$ are independent with each other. The dynamic model for graph motion is as follows:

$$p(G_t|G_{t-1};\Theta_{dyn}) = \qquad (8)$$
$$\prod_{i=1}^{3} p(l_{i,t}|l_{i,t-1}) \cdot \prod_{i=1}^{3} p(T_{i,t}^{geo}|T_{i,t-1}^{geo}) \cdot \prod_{i=1}^{3} p(T_{i,t}^{pht}|T_{i,t-1}^{pht})$$

where, Θ_{dyn} is the parameters accounting for aforementioned two types of variations in the motion of the graph chain and is learned from the training data. The continuous variation transition model can be represented as follows for all the three resolutions.

$$p(T_{i,t}^{geo}|T_{i,t-1}^{geo}) \quad \propto \quad \exp(-\mathcal{D}^{geo}(T_{i,t}^{geo}, T_{i,t-1}^{geo})) \quad (9)$$
$$p(T_{i,t}^{pht}|T_{i,t-1}^{pht}) \quad \propto \quad \exp(-\mathcal{D}^{pht}(T_{i,t}^{pht}, T_{i,t-1}^{pht})) \quad (10)$$

where $\mathcal{D}^{geo}$ and $\mathcal{D}^{pht}$ are the predefined geometric and photometric distance.

We denote by $I[1,\tau]$ and $G[1,\tau]$ the image and graph sequences respectively for a period $[1,\tau]$. Therefore, our overall probabilistic model is a joint probability

$$p(I[1,\tau], G[1,\tau]; \Theta) \qquad (11)$$
$$= \prod_{t=1}^{\tau} p(I_t|G_t; \Theta_{img,t}) \cdot p(G_1) \cdot \prod_{t=2}^{\tau} p(G_t|G_{t-1}; \Theta_{dyn})$$

Here $\Theta = \{\Theta_{img,t}, \Theta_{dyn}\}$ is the parameter that drives the overall probabilistic model. $p(I_t|G_t; \Theta_{img,t})$ is the image model, which generates an image from a graph G_t with $\Theta_{img,t}$ being the parameters (including the dictionaries at different layers). $p(G_t|G_{t-1}; \Theta_{dyn})$ is the dynamic model for the motion of graphs at different ages with Θ_{dyn} being the motion (aging) parameters.

2.3. Face Aging Simulation

According to the multilayer representation, we simulate face aging at 3 layers separately. Facial component aging and wrinkle addition are the key points of our work.

To overcome the difficulty of collecting the photos of a person at different age groups, we collect a set of face components of different types for each age group. For each sample in $\Delta_{i,t}$ we label the contour shape as displayed in Fig.4 (b). Then for each component image pair $[\Delta_{i,t}(j), \Delta_{i,t-1}(k)]$ within two consecutive age groups in the dictionary, we define a geometric distance $\mathcal{D}_t^{geo}(j,k)$ and a photometric distance $\mathcal{D}_t^{pht}(j,k)$ to measure the similarity between them. Fig.4(a) gives an example of the training set and the matches.

(1) Global Appearance Aging

For the whole face aging, we just select an aged image with proper face type from $\Delta_{fc,t}$, and use simple merge technique to reflect the change of face shape, skin color darkening and drops of muscles. Shape context warping is adopted to warp proper hair style from $\Delta_{hair,t-1}(j)$ to $\Delta_{hair,t-1}(k)$. Artifacts along the edges are blurred. Therefore, the transition probability is defined as

$$
\begin{aligned}
& p(l_{1,t}|l_{1,t-1}) \qquad\qquad\qquad (12) \\
= \; & p(l_{1,t}^{fc}=j'|l_{1,t-1}^{fc}=k') \cdot p(l_{1,t}^{hair}=j|l_{1,t}^{hair}=k) \\
\propto \; & \exp(-(\mathcal{D}_{hair}^{geo}(j,k)+\mathcal{D}_{fc}^{pht}(j',k')+\mathcal{D}_{fc}^{geo}(j',k')))
\end{aligned}
$$

(2) Face Component Aging

In the image model at this layer, $l_{2,t}$ is the switch variable for the alternatives of the face components at age t, the abrupt variation takes place when the switch variable changes value by jumping from $\Delta_{2,t-1}(k)$ to $\Delta_{2,t}(j)$. Therefore, the transition dynamics can be written as follows:

$$
p(l_{2,t}=j|l_{2,t-1}=k) \propto \exp(-(\mathcal{D}_t^{geo}(j,k)+\mathcal{D}_t^{pht}(j,k))) \quad (13)
$$
$$
j=1,2,...,N_t, k=1,2,...,N_{t-1}
$$

N_t and N_{t-1} are the numbers of components in $\Delta_{cmp,t}$ and $\Delta_{cmp,t-1}$ respectively.

By sampling from the dynamic model at this layer, we can get $w_{2,t}$, and the aged component image $I_{2,t}$ can be synthesized by Eq.6. An example of eye aging is displayed in Fig.4 (c).

(3) Wrinkles Addition

For wrinkle addition, we decompose face into 8 zones, as is shown in Fig.5 (a), and add wrinkles for each zone separately. Collecting the wrinkle images of a person across a sequence of age groups is impractical. Therefore, we collect a large number of face images at different age groups, and use the statistical data instead. In our approach, we model the number of wrinkles with Poisson distribution.

$$
p(N_t=k) = \frac{\exp(-\lambda_t)(\lambda_t)^k}{k!} \quad (14)
$$

where N_t is the number of wrinkles at age group t, λ_t is the parameter for the distribution, which can be learned from
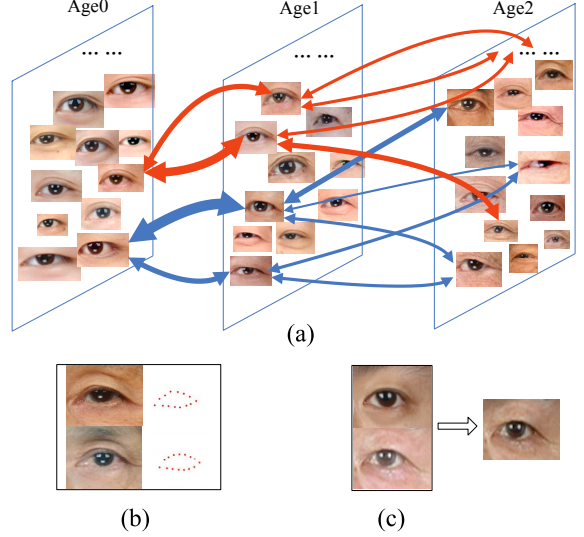

(a)

(b)   (c)

Figure 4. (a) give sample set of eye at three age range. The arrows between the matches between eyes at two sequent age, and the thickness of the arrows indicate the probabilities of eye aging.(b) is the labeled landmarks of two eye match (c) is one aging result of a young eye.
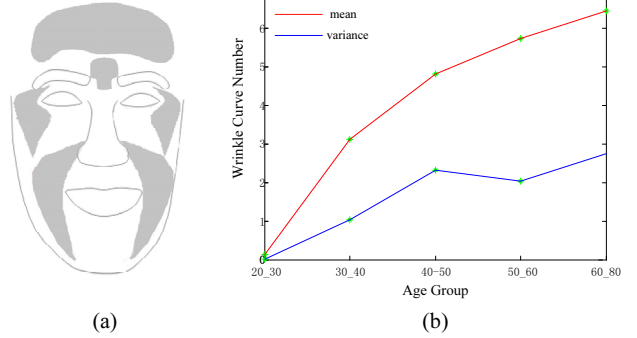

(a)   (b)

Figure 5. Facial zones and statistic of forehead wrinkle number

the training data as below. Fig.6(a) displays several examples of the training data.

$$
\lambda_t = \frac{1}{M_t}\sum_{i=1}^{M_t} N_t^i \quad (15)
$$

where M_t is the number of training images at age group t and N_t^i is the wrinkle number of the ith sample at age group t.

It should be noted that the geometric variable $T_{3,t}^{geo}$ here describes the geometry of the wrinkle curves, including the number, positions, orientations, and scales. The wrinkle number can be sampled from Eq.14. The other variables can be sampled from the corresponding prior distributions. Fig.6(b) is a sequence of wrinkle group generated by $T_{3,t}^{geo}$.

The transition probability of the switch variable $l_{3,t}$ is similar to the other parts. However, because only the wrinkle texture is selected across age groups, the transition only has the photometric distance while the geometric change is

| 30-40 | 40-50 | 50-60 | 60-80 |

(a)
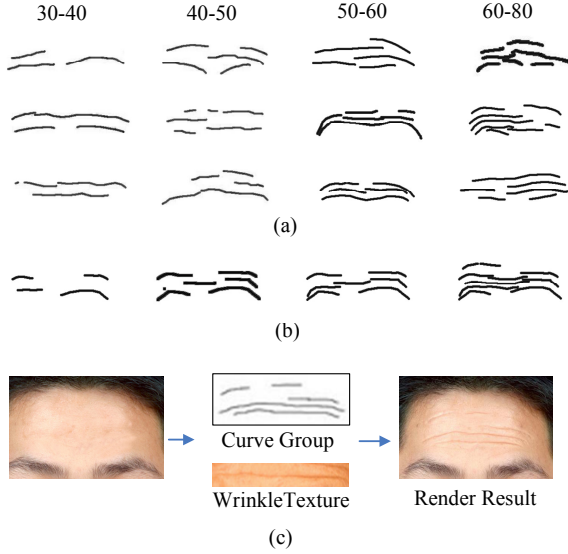
(b)

Curve Group

WrinkleTexture   Render Result

(c)

Figure 6. (a) is some curve groups(in forehead zone) labeled from training data and (b) shows some synthesized wrinkle curve groups. (c) is one example of wrinkle addition process.

already incorporated in $p(T_{3,t}^{geo}|T_{3,t-1}^{geo})$.

$$p(l_{3,t} = j|l_{3,t-1} = k) \propto \exp(-\mathcal{D}_t^{pht}(j,k)) \qquad (16)$$

Given the wrinkle groups, the realistic images, with wrinkle added, can be synthesized according to Eq. 6 using the wrinkle texture examples and the process is shown in Fig.6(c).

3. Computing and Simulation

3.1. Flow of Algorithm

Step 1) Compare with the input image I_1, and build the initial graph G_1 at start age point.

$$G_1 = \arg\max p(I_1|G_t; \Theta_{img,t})$$

Step 2) For $t = 2, 3, ..., \tau$

    1. Sample the graph G_t from three items in Eq.9
       $G_t \sim p(G_t|G_{t-1}; \Theta_{dyn})$

    2. Synthesize the aged image I_t from learned parameter $\Theta_{img,t}$ and G_t.
       $I_t = J^{rec}(G_t; \Delta_t)$

3.2. Variabilities of aging results

The motion of Markov chain is probabilistic. G_t and I_t are sampled from the generative models. Similar to the Brownian motion, the longer the time period, the higher variance is observed in the sample results. This is illustrated in our experimental result shown in Fig.7. For each input face, we can sample a number of plausible aged faces over time. We sample more images as time goes by.
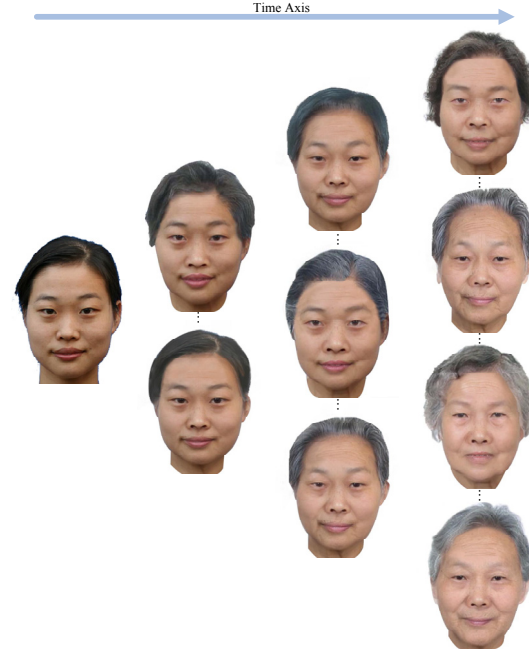

Figure 7. The uncertainty of aging result increases with time.

4. Experiment

4.1. Data collection

There are two sources of aging database in our experiment. One is the FG-Net aging database[24]. The other is the database we collected ourselves. Our database includes 50,000 mid-resolution images of subjects at different age groups.

The landmarks accounting for the profile and the wrinkles are manually labeled by the artists. According to these labeled data we get the statistic of shape parameters and wrinkle groups, from which we get the aging pattern and synthesize the final aged image. Some face aging results are displayed in Fig.9.

4.2. Two Quantitative studies

To verify the validity of our model and aging approach, we conducted two experiments here. We divide ages into 5 age groups:20-30, 30-40, 40-50, 50-60 and 60-80. We select 20 young faces aged 20-30, for each one, 4 aged images belong to four groups above 30 respectively are synthesized. Twenty testees are asked to evaluate the aging results.

In the First Experiment. We present the testees with two image set **A** and **B**. Set **A** includes the 80 synthesized images and Set **B** includes the same number of real images. Both set **A** and **B** have 20 images in each age group above 30. Then the testees are asked to estimate the age group of the faces in Set **A** and Set **B** separately. The estimation results are displayed in Fig.8.

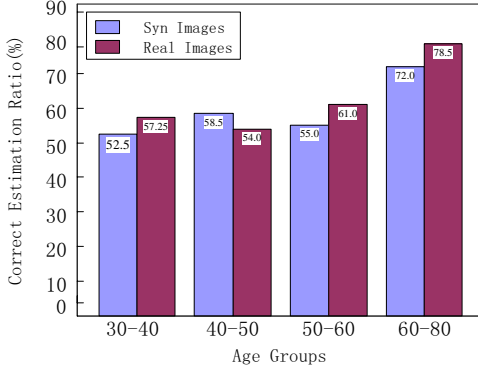The experimental results show that our model and statis-

Figure 8. Age estimation of synthesized images and real images.

tical data contain most of the age related variations at each age point, and the aging results are consistent with the human perception in a large extent.

In the second Experiment, we give the testees two image sets **A** and **B**. Set **A** contains 50 face images aged between 20 and 30, including the 20 young faces we aged. Set **B** contains the 80 synthesized images. For each face in **B** we ask them to match its young face in **A**, the rate of right matching is shown in Table 1.

Table 1. **Correct matching rate of the synthesized face images.**

Age Group	30-40	40-50	50-60	60-80
Correct Matching(%)	100	83.21	75.58	50.71

The experimental result shows that our approach is subject specific, it retains the identity information of the young image. But the recognition rate decrease with age increase, it indicates that simulating face aging effects would become more challenging with the time range increases.

5. Discussion

There are a few important factors that we have learned in this study. (i) A large training set is the key. Currently our annotated dataset is limited to Asian faces, but we are extending this to other ethnic groups. (ii) Global appearance, such as hair color and hair style has large influence on photorealism and age perception. This is an important factor contributing to our success. (iii) 3D head and muscle models will be important to model the deformation for senior faces (60-80 years old). This part is beyond our 2D model. But it is still possible to overcome this problem by collecting senior face images. (iv) More experiments are needed to quantify the variance in face aging and to validate the aging model.

6. Acknowledgement

References

[1] Z. J. Xu, H. Chen, S. C. Zhu, "A high resolution grammatical model for face representation and sketching". *CVPR*,2005. 1, 2, 3

[2] A. Lanitis, C. J. Taylor, and T. F. Cootes, "Toward automatic simulation of aging effects on face images", *IEEE Trans. on PAMI*, vol.24, n.4, p.442-455, 2002. 1

[3] J. B. Pittenger and R. E. Shaw, "Aging faces as viscal-elastic events: implications for a theory of nonrigid shape perception", *Journal of Experimental Psychology:Human Perception and Performance*.1(4):374C382, 1975. 1

[4] N. Ramanathan, R. Chellappa, "Modeling age progression in young faces", *CVPR*,2006. 1

[5] N. Ramanathan and R. Chellappa, "Face verification across age progression", *CVPR,2005* 1

[6] L. S. Mark, J. T. Todd and R. E. Shaw, "Perception: a geometric analysis of how different styles of changes are distinguished", *Journal of Experimental Psychology Perception and Performance*, 7:855-868,1981. 1

[7] M. Gandhi, "A method for automatic synthesis of aged human facial images", Master's thesis, McGill University,2004. 1

[8] D. M. Burt and D. I. Perrett, "Perception of age in adult caucasian male faces computer graphic manipulation of shape and color information", *Proc. Royal Soc. London*, vol.259,1995. 1

[9] D. A. Rowland and D. I. Perrett, "Manipulating facial appearance through shape and color", *IEEE Trans. Computer Graphics and Applications*,1995. 1

[10] B. P. Tiddeman, D. M. Burt and D. I. Perrett, "Prototyping and transforming facial textures for perception research", *IEEE Trans. Computer Graphics and Applications*,2001. 1

[11] B. P. Tiddeman, M. Stirrat, and D. I. Perrett, "Towards realism in facial prototyping: results of a wavelet MRF method", *Proc. Theory and Practice of Computer Graphics*,2006 1

[12] Y. Shan and Z. Y. Zhang, "Image based surface detail transfer", *IEEE Trans. CVPR*,2001. 1

[13] F. R. Leta et al., "Manipulating facial appearance through age parameters", *SIGGRAPH*,1996. 1

[14] A. Golovinskiy et al., "A statistical model for synthesis of detailed facial geometry", *ACM Trans. on Graphics*,2006. 1

[15] L. S. Mark et al., "Wrinkling and head shape as coordinated sources of age level information", *Journal Perception Psychophysics,27(2):117-124,1980*. 1
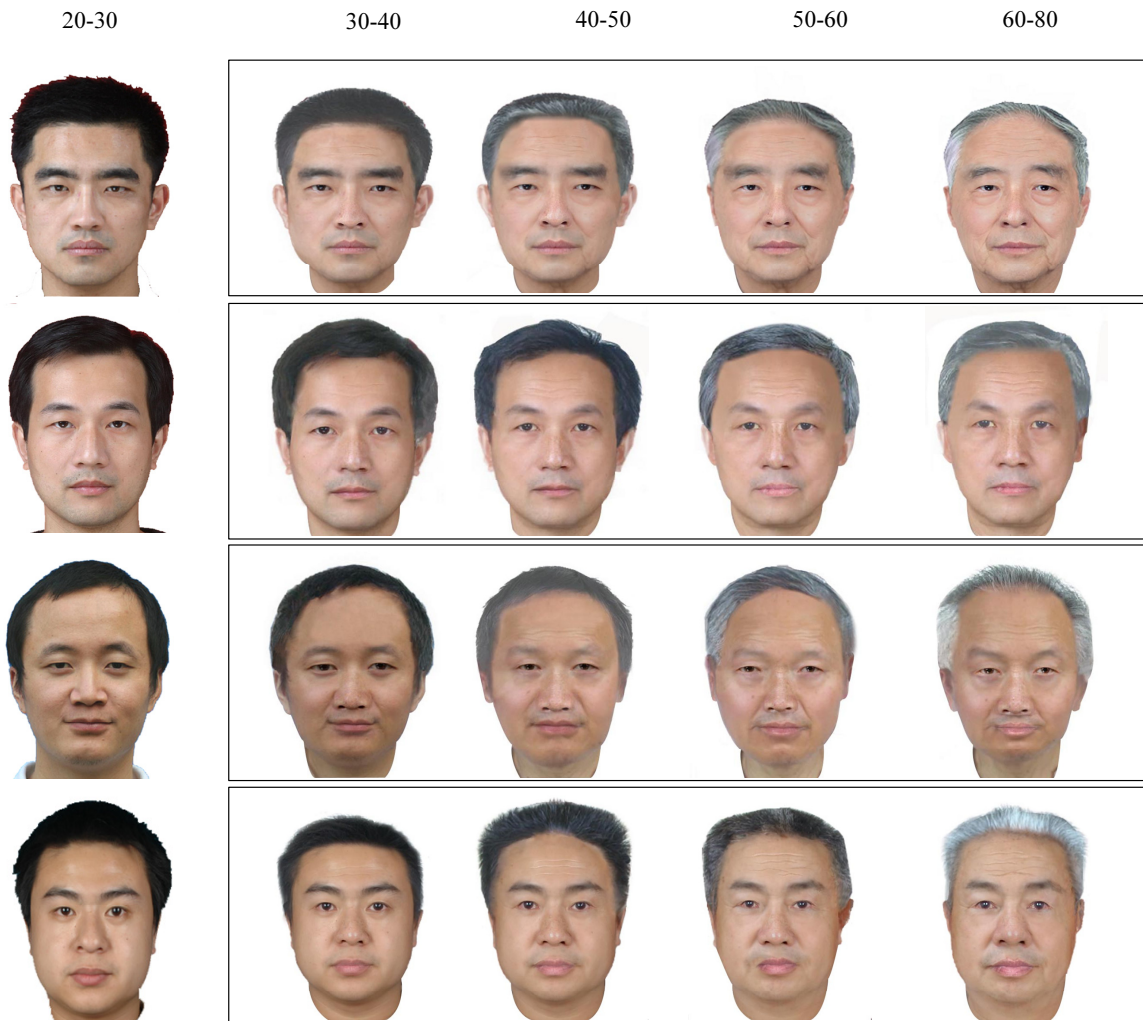
Figure 9. Some more aging result. The leftmost column is the original images of the subjects. The 2nd to 5th row are synthesized aged images at 4 age groups respectively.

[16] Y. Wu, P. Beylot, and N. M. Thalmann, "Skin Aging Estimation by Facial Simulation", *Proc. of the Computer Animation*,1999. 1

[17] Y. Wu, N. M. Thalmann, and D. Thalmann, "A Dynamic Wrinkle Model in Facial Animation and Skin Aging", *Journal of Visualization and Computer Animation, 1995*, 6:195-205,1995. 1

[18] L. Boissieux et al., "Simulation of skin aging and wrinkles with cosmetics insight", *Computer Animation and Simulation*,2000. 1

[19] A. C. Berg, "Aging of Orbicularis Muscle in Virtual Human Faces", *International Conference on Information Visualization*,2003. 1

[20] Y. H. Kwon and N. da Vitoria Lobo, "Age classification from facial images". *Computer Vision and Image Understanding*,1999. 1

[21] A. Lanitis, C. Dragonova and C. Christondoulou, "Comparing Different Classifiers for Automatic Age Estimation". *IEEE Trans. on Systems, Man and Cybernetics*,2004. 1

[22] L. G. Farkas, *Anthropometry of the Head and Face*, Raven Press, New York, 1994. 1

[23] L. G. Farkas and I. R. Munro. *Anthropometric Facial Proportions in Medicine*, Charles C. Thomas, Springfield, Illinois, USA,1987. 1

[24] "Face and Gesture Recognition", Network: FG-NET aging database. [online] Available:(http://sting.cycollege.ac.cy/ alanitis/fgnetaging/). 6

[25] Y.Z. Wang and S.C. Zhu. "Modeling complex motion by tracking and editing hidden Markov graphs", *CVPR*,2004. 3

[26] J.Y.Wang, Y.Shang etc. "Age simulation for face recognitions", *ICPR*,2006. 1

[27] Hill CM, Solomon CJ, Gibson SJ. "Aging the human face-A statistically rigorous approach", *ICDP*,2005. 1

[28] Z.Y.Yao, X.Yang, S.C.Zhu. "Introduction to a Large-Scale General Purpose Ground Truth Database: Methodology, Annotation Tool and Benchmarks", *EMMCVPR*,2007. 7